Proc. Budapest'02 Workshop on
Quark & Hadron Dynamics (2002) 000–000

Budapest'02 Workshop on
Quark & Hadron Dynamics
Budapest, Hungary
March 3–7, 2002

Resummed pQCD for $W^{\pm}$ and Z^0 transverse momentum spectra at RHIC and LHC

Xiaofei Zhang[1] and George Fai[1]

[1] Center for Nuclear Research, Department of Physics, Kent State University
Kent, Ohio 44242, USA

Abstract. We predict $W^{\pm}$ and Z^0 transverse momentum distributions from proton-proton and nuclear collisions at RHIC and LHC. A resummation formalism with power corrections to the renormalization group equations is used. Shadowing effects are discussed and found to be unimportant at RHIC, but important for LHC. We study the enhancement of power corrections due to multiple scattering in nuclear collisions and numerically illustrate the weak effects of the dependence on the nuclear mass.

Keywords: gauge boson, resummed, transverse momentum
PACS: PACS Numbers: 25.75.-q, 25.75.Dw, 24.85.+p, 14.70.-e, 12.38.Cy

1. Introduction

With RHIC running at the full energy, and experiments at the Large Hadron Collider (LHC) at several TeV/nucleon soon to follow, "clean" processes, where pQCD works well in pp collisions, are needed to test pQCD in nuclear reactions at collider energies. It is particularly important to distinguish between expected nuclear effects and "new physics".

The production of $W^{\pm}$ and Z^0 bosons has been extensively studied at Tevatron energy ($\sqrt{s} = 1.8$ TeV). Perturbative QCD proved to be very successful in explaining the CDF[1] and D0[2] data. Due to the large mass of $W^{\pm}$ and Z^0, and no final state rescattering in their production process, power corrections are expected to be small. Therefore, $W^{\pm}$ and Z^0 production could provide a bench mark test for pQCD at RHIC and LHC in both pp and nuclear collisions.

The bulk of the data for $W^{\pm}$ and Z^0 production is concentrated in the small transverse momentum (p_T) region, where p_T is much smaller than the corresponding gauge boson mass (M). When $p_T \ll M$, the p_T distributions calculated order-by-order in α_s in conventional fixed-order perturbation theory receive a large logarithm, $\ln(M^2/p_T^2)$, at every power of α_s, even in the leading order in α_s. Therefore, at sufficiently small p_T, the convergence of the conventional perturbative expansion in powers of α_s is impaired, and the logarithms must be resummed.

In this talk, we will first introduce the recent development of the resummation theory in addition to the original $\tilde{b}$ space resummation theory which was proposed by Collin, Sopper and Sterman (CSS). We will use the new formalism with power correction to the evolution equation to predict the $W^{\pm}$ and Z^0 production at RHIC and LHC. We will also discuss the nuclear effects on massive gauge boson transverse momentum distributions. These effects include both the nuclear modification of the parton distribution function (shadowing), and the initial state power corrections.

2. Collins-Soper-Sterman (CSS) formalism and improved extrapolation formula with power corrections

In the production of gauge bosons (of mass M), when $p_T \ll M$, the p_T distribution calculated order-by-order in α_s in conventional fixed-order perturbation theory receives a large logarithm, $\ln(M^2/p_T^2)$, at every power of α_s. Even at the leading order in α_s, the cross section $d\sigma/dM^2\,dy\,dp_T^2$ contains a term proportional to $(\alpha_s/p_T^2)\ln(M^2/p_T^2)$ coming from the partonic subprocess $q+\bar{q}\rightarrow V+g$, where $V=\gamma^*, W^{\pm}$ or Z^0. Beyond the leading order, we actually get two powers of the logarithm for every power of α_s, due to soft and collinear gluons emitted by the incoming partons. Therefore, at sufficiently small p_T, the convergence of the conventional perturbative expansion in powers of α_s is impaired, and the logarithms must be resummed.

For vector boson production in hadronic collisions between hadrons h_A and h_B, $h_A+h_B\rightarrow V(M)+X$ with $V=\gamma^*, W^{\pm}$, or Z^0, the CSS resummation formalism yields the following generic form [4]:

$$\frac{d\sigma(h_A+h_B\rightarrow V+X)}{dM^2\,dy\,dp_T^2}=\frac{1}{(2\pi)^2}\int d^2\tilde{b}\,e^{i\vec{p}_T\cdot\vec{\tilde{b}}}\,\tilde{W}(\tilde{b},M,x_A,x_B)+Y(p_T,M,x_A,x_B)\ , \tag{1}$$

where $x_A=e^{y}\,M/\sqrt{s}$ and $x_B=e^{-y}\,M/\sqrt{s}$, with rapidity y and collision energy $\sqrt{s}$. In Eq. (1), the $\tilde{W}$ term dominates the p_T distributions when $p_T \ll M$, and the Y term gives corrections that are negligible for small p_T, but become important when $p_T \sim M$.

In the CSS formalism, the function $\tilde{W}$ appears as a superposition,

$$\tilde{W}(\tilde{b},M,x_A,x_B)=\sum_{ij}\tilde{W}_{ij}(\tilde{b},M,x_A,x_B)\,\sigma_{ij\rightarrow V}(M)\ , \tag{2}$$

where $\sigma_{ij\rightarrow V}(M)$ is the lowest order cross section for a quark-antiquark pair of invariant mass M to annihilate into a vector boson V, and the $\sum_{ij}$ runs over all possible quark and antiquark flavors that can annihilate into the vector boson at the Born level[4]. In Eq. (2), $\tilde{W}_{ij}(\tilde{b},M,x_A,x_B)$ is an effective flux to have partons of flavor i and j from the respective hadrons h_A and h_B, and it has the form

$$\tilde{W}_{ij}(\tilde{b},M,x_A,x_B)=\mathrm{e}^{S(\tilde{b},M)}\,\tilde{w}_{ij}(\tilde{b},c/\tilde{b},x_A,x_B)\ , \tag{3}$$

where $S(\tilde{b}, M)$ is given in the Sudakov factor, and c is a constant of order unity[4,5]. The functions $\tilde{w}_{ij}(\tilde{b}, c/\tilde{b}, x_A, x_B)$ in Eq. (3) depend on only one momentum scale, $1/\tilde{b}$, and are perturbatively calculable as long as $1/\tilde{b}$ is large enough. All large logarithms from $\ln(1/\tilde{b}^2)$ to $\ln(M^2)$ in $\tilde{W}_{ij}(\tilde{b}, M, x_A, x_B)$ are completely resummed into the exponential factor $\exp[S(\tilde{b}, M)]$.

Since the perturbatively resummed $\tilde{W}_{ij}(\tilde{b}, M, x_A, x_B)$ in Eq. (3) is only reliable for the small $\tilde{b}$ region, an extrapolation to the large $\tilde{b}$ region is necessary in order to complete the Fourier transform in Eq. (1). In the original CSS formalism, a variable $\tilde{b}_*$ and a nonperturbative function $F^{NP}_{CSS}(\tilde{b}, M, x_A, x_B)$ were introduced[4] in such a way that $\tilde{W}$ was modified for all $\tilde{b}$ (except $\tilde{b} = 0$) as

$$\tilde{W}^{\rm CSS}(\tilde{b}, M, x_A, x_B) \equiv \tilde{W}(\tilde{b}_*, M, x_A, x_B)\, F^{NP}_{CSS}(\tilde{b}, M, x_A, x_B)\,, \tag{4}$$

where $\tilde{b}_* = \tilde{b}/\sqrt{1 + (\tilde{b}/\tilde{b}_{max})^2}$, with $\tilde{b}_{max} = 0.5$ GeV^{-1}. This construction ensures that $\tilde{b}_* \leq \tilde{b}_{max}$ for all values of $\tilde{b}$. The function F^{NP}_{CSS} is a Gaussian in $\tilde{b}$, $F^{NP}_{CSS} \sim \exp(-\kappa \tilde{b}^2)$ with κ having a certain M^2, x_A, and x_B dependence[4].

The original CSS extrapolation introduces a modification to the perturbative calculation, and the size of the modifications depends on the non-perturbative parameters in $F^{NP}_{CSS}(\tilde{b}, M, x_A, x_B)$. In oder to improve the predictive power of the CSS $\tilde{b}$-space resummation formalism, the following new form was proposed[5] by solving the renormalization group equation including power corrections:

$$\tilde{W}(\tilde{b}, M, x_A, x_B) = \begin{cases} \tilde{W}(\tilde{b}, M, x_A, x_B) & \tilde{b} \leq \tilde{b}_{max} \\ \tilde{W}(\tilde{b}_{max}, M, x_A, x_B)\, F^{NP}(\tilde{b}, M, x_A, x_B; \tilde{b}_{max}, \alpha) & \tilde{b} > \tilde{b}_{max} \end{cases}\,, \tag{5}$$

where the nonperturbative function F^{NP} in Eq. (5) is given by

$$\begin{aligned} F^{NP}(\tilde{b}, M, x_A, x_B; \tilde{b}_{max}, \alpha) \; = \; & \exp\Bigg\{ - \ln\left(\frac{M^2 \tilde{b}^2_{max}}{c^2}\right) \Big[g_1 \left((\tilde{b}^2)^\alpha - (\tilde{b}^2_{max})^\alpha \right) \\ & + g_2 \left(\tilde{b}^2 - \tilde{b}^2_{max} \right) \Big] - \bar{g}_2 \left(\tilde{b}^2 - \tilde{b}^2_{max} \right) \Bigg\}\,. \end{aligned} \tag{6}$$

In Eq. (5) $\tilde{b}_{max}$ is a parameter to separate the perturbatively calculated part from the non-perturbative input. Unlike in the original CSS formalism, when $\tilde{b} \leq \tilde{b}_{max}$, the perturbatively calculated $\tilde{W}(\tilde{b}, M, x_A, x_B)$ is not altered and is independent of the nonperturbative parameters. In addition, the $\tilde{b}$-dependence in Eq. (6) is separated according to different physics origins. The coefficients g_1 , g_2 and $\bar{g}_2$ are looked upon in the present work as fitting parameters, The values of g_1 and α are fixed by the requirement of continuity. The $(\tilde{b}^2)^\alpha$-dependence mimics the summation of the perturbatively calculable leading power contributions to all orders in the running coupling constant $\alpha_s(\mu)$ with the scale μ running into the non-perturbative region [11]. The $\tilde{b}^2$-dependence of the g_2 term is a direct consequence of dynamical power corrections to the renormalization group equations, and has an explicit dependence on M. The $\bar{g}_2$ term represents the effect of the non-vanishing intrinsic parton transverse momentum. As we discuss later, these two terms behave differently in nuclear collisions.

A remarkable feature of the $\tilde{b}$-space resummation formalism is that the resummed exponential factor $\exp[S(\tilde{b},M)]$ (see Eq. (3)) suppresses the $\tilde{b}$-integral when $\tilde{b}$ is larger than $1/M$. In fact, it was shown using the saddle point method that, for a large enough M, a QCD perturbation calculation is valid even at $p_T = 0$[12, 4]. As discussed in Ref. [5], the value of the saddle point strongly depends on the collision energy $\sqrt{s}$, in addition to its well-known M^2 dependence. Because of the steep evolution of parton distributions at small x, the $\sqrt{s}$ dependence of the $\tilde{W}$ in Eq. (1) significantly decreases the value of the saddle point and improves the predictive power of the $\tilde{b}$-space resummation formalism at collider energies.

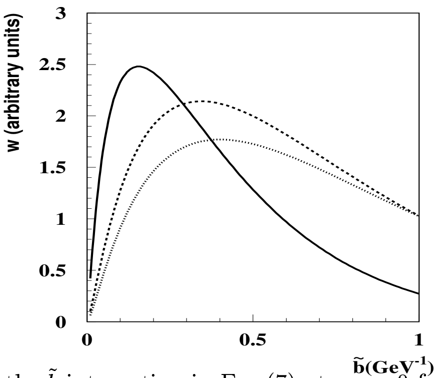

Fig. 1. Integrand of the $\tilde{b}$-integration in Eq. (7) at $p_T = 0$ for Z^0 as a function of $\tilde{b}$ with an arbitrary normalization at $\sqrt{s} = 350$ GeV (dotted line), $\sqrt{s} = 500$ GeV (dashed), and $\sqrt{s} = 5.5$ TeV (solid).

To display the saddle point clearly, let us rewrite the first term on the right-hand side of Eq. (1), taking into account that there is no preferred transverse direction and that $\tilde{W}$ in Eq. (1) is a function of $\tilde{b} = |\vec{\tilde{b}}|$ only:

$$\frac{1}{(2\pi)^2}\int d^2\tilde{b}\, e^{i\vec{p}_T\cdot\vec{\tilde{b}}}\, \tilde{W}(\tilde{b},M,x_A,x_B) = \frac{1}{2\pi}\int_0^\infty d\tilde{b}\, J_0(p_T\tilde{b})\, W(\tilde{b},M,x_A,x_B)\ , \quad (7)$$

where $J_0(z)$ with $z = p_T\tilde{b}$ represents the Bessel function of order zero. Figure 1 is a graph (on an arbitrary scale) of the integrand I of the right hand side of Eq. (7) with $p_T = 0$ for the case of Z^0 production at the collision energies where we intend to carry out our calculations: $\sqrt{s} = 350$ GeV (dotted line), $\sqrt{s} = 500$ GeV (short dashes), and at $\sqrt{s} = 5.5$ TeV (solid). The position of the saddle point decreases as the collision energy increases.

3. Gauge boson production in *pp* collisions

As mentioned above, the parameters g_1 and α of Eq. (6) are fixed by the requirement of continuity of the function $\tilde{W}(\tilde{b})$ and its derivative at $\tilde{b} = \tilde{b}_{max}$. We use $\tilde{b}_{max} = 0.5$ GeV^{-1} in Ref. [5] and here.) The value of g_2 and $\bar{g}_2$ can be obtained by fitting the low-energy Drell-Yan data, and are taken to be $\bar{g}_2 \sim 0.27$ GeV^2, and $g_2 \sim 0.01$ GeV^2 following Refs. [5] and [13]. As the $\tilde{b}$ dependence of the g_2 and $\bar{g}_2$ terms in Eq. (6) is identical, it is convenient to combine these terms and define

$$G_2 = \ln(\frac{M^2 \tilde{b}_{max}^2}{c^2}) g_2 + \bar{g}_2 \quad . \tag{8}$$

Using the values of the parameters listed above, we get $G_2 \sim 0.4$ GeV^2 for $W^{\pm}$ and Z^0 production in *pp* collisions. Our results are not sensitive to small variations of G_2 around its estimated value. We use $G_2 = 0.4$ GeV^2 in the following. An impression about the importance of power corrections can be obtained by comparing results with $G_2 = 0.4$ GeV^2 to those with power corrections turned off ($G_2 = 0$). We therefore define the ratio of these quantities:

$$R_{G_2}(p_T) \equiv \frac{d\sigma^{(G_2)}(p_T)}{dp_T} \Bigg/ \frac{d\sigma(p_T)}{dp_T} \quad . \tag{9}$$

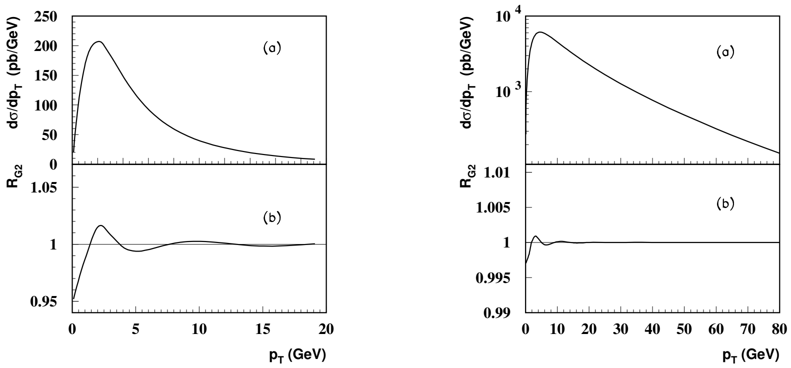

Fig. 2. (a) Cross section $d\sigma/dp_T$ for $W^{\pm}$ production in *pp* collisions. (b) R_{G_2} defined in Eq. (9) for $W^{\pm}$ at the same energy. the left is for RHIC with$\sqrt{s} = 500$ GeV; the right is for LHC with$\sqrt{s} = 14$ TeV;

In the left panel of Figure 2(a) we show the differential cross section for $W^{\pm}$ production (In what follows, by $W^{\pm}$ production cross section we mean the cross section for $W^{+} + W^{-}$.) in *pp* collisions at $\sqrt{s} = 500$ GeV, where a RHIC *pp* run is expected. The accompanying Figure 2(b) displays R_{G_2} of Eq. (9). It can be seen that the R_{G_2} ratio converges to unity (i.e. very small power corrections) with increasing p_T, and the effect of power corrections is about five percent for $p_T = 0$. However, when $p_T > 2$ GeV, the deviation of R_{G_2} from unity is under two percent.

The right panel of Figures 2 contains similar information for $W^{\pm}$ production in pp collisions at the planned LHC nucleus-nucleus collision energy of $\sqrt{s} = 14$ TeV. At all energies, the magnitude of the $W^{\pm}(= W^+ + W^-)$ production cross section is about 3 to 5 times that of the Z^0 production cross section. Otherwise, the results for Z^0 and $W^{\pm}$ production are very similar. Therefore we only present the figures for $W^{\pm}$.

As expected from Figure 1, the dependence on the nonperturbative input decreases with increasing collision energy. The R_{G_2} ratio is smaller than one percent at LHC for both $\sqrt{s} = 5.5$ TeV and $\sqrt{s} = 14$ TeV, even when $p_T = 0$. These results confirm that the predictive power of the formalism is very good at RHIC and excellent at LHC. They also show that the effect of power corrections is very small at LHC for almost the whole p_T region and it is also negligible for RHIC when p_T is larger than 2 GeV.

4. Isospin and shadowing effects in nuclear collisions

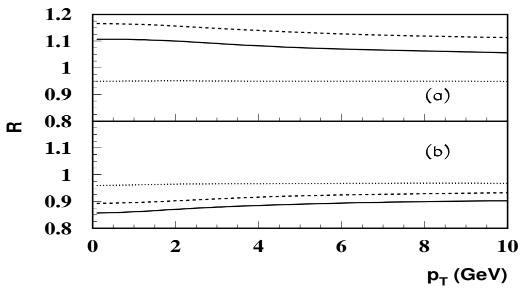

Fig. 3. (a) The isospin ratio, R_{iso}, defined in Eq. (10) (dashed line), the shadowing ratio, R_{sh}, defined in Eq. (11) (solid line), and "pure shadowing" (dotted) for Z^0 in $p + Au$ collisions at $\sqrt{s} = 350$ GeV; (b) same as (a) for $W^{\pm}$ production.

As the parton distribution of neutrons is different from that of the protons, the production cross section of gauge bosons in proton-neutron and neutron-neutron interactions differs from the corresponding production cross section in pp collisions. This difference is the source of the so-called isospin effects. To study the isospin effects, let us introduce

$$R_{iso}(p_T) \equiv \frac{d\sigma(p_T, Z_A/A, Z_B/B)}{dp_T} \bigg/ \frac{d\sigma(p_T)}{dp_T} \ , \tag{10}$$

where Z_A and Z_B are the atomic numbers and A and B are the mass numbers of the colliding nuclei, and the cross section $d\sigma(p_T, Z_A/A, Z_B/B)/dp_T$ has been averaged over AB, while $d\sigma(p_T)/dp_T$ is the pp cross section (with $G_2 = 0$).

Next we turn to the phenomenon of shadowing. We use the term shadowing in the general sense, referring to all modifications of the parton distribution function in the environment of the nucleus[8]. There are several different parameterization of shadowing [16–19]. In this work, we focus more attention on scale dependence, we find the original EKS98 shadowing parameterization most appropriate for our present purposes. Therefore we use EKS98 shadowing[18] in this work.

Similarly to Eq. (10) for isospin effects, we define a shadowing ratio,

$$R_{sh}(p_T) \equiv \frac{d\sigma^{(sh)}(p_T, Z_A/A, Z_B/B)}{dp_T} \Bigg/ \frac{d\sigma(p_T)}{dp_T} \ . \tag{11}$$

Thus, R_{sh} incorporates the effects of both shadowing and the isospin composition of the nuclei. Furthermore, in this Section we take $G_2 = 0$ throughout, switching off power corrections. The enhanced power corrections in pA and AB collisions will be discussed separately in the next Section.

Figure 3 displays R_{iso} (dashed lines) and R_{sh} (full lines) as functions of p_T for Z^0 production (Figure 3(a)) and $W^{\pm}$ production (Figure 3(b)), respectively, at $\sqrt{s} = 350$ MeV. The same information is presented at $\sqrt{s} = 5.5$ TeV in Figure 4. At LHC, $x \sim 0.02$, and the magnitude of the isospin effects is about 2%. This is because when x is in this range, the difference of the distributions of $u(\bar{u})$ and $d(\bar{d})$ quarks in the nucleus is very small. At RHIC, where the dominant $x \sim 0.26$, the isospin effects are about 20% in the small p_T region. We have also checked that the scale dependence of isospin effects is not important. In Figure 3, we also show a dotted line, which is the ratio of R_{sh} to R_{iso}, and thus can be considered to display the effect of "pure shadowing". Pure shadowing appears as an approximately constant reduction of 3-5% at $x \sim 0.26$.

The appearance of R_{sh} (full lines) is more surprising at $\sqrt{s} = 5.5$ TeV (Figure 4). Since at LHC, even at $p_T = 80$ GeV, $x \sim 0.04$, we are still in the "strict shadowing" region. Therefore, the fact that $R_{sh} > 1$ for 20 GeV $< p_T <$ 70 GeV is not "anti-shadowing"; rather, it is a consequence of the change of the shape of the cross section from pp to AB reactions. In pp collisions, the maximum of the cross section is at $p_T \approx 3.7$ GeV. In AB collisions, the peak is shifted by about 0.4 GeV in the direction of large transverse momenta. On the other hand, the contributions from the scale $\mu \sim p_T$ to M have been resummed. Resummation plays a more important role for small p_T than for large p_T. In EKS98, the strict shadowing effect is more important for small scales, such as $p_T \sim 2 - 5$ GeV, than for $p_T \sim M$. Thus, a relatively small shift in the peak position brings about the rise of R_{sh} above unity. The shadowing ratio R_{sh} dips below one again at a certain p_T, to approach the fixed-order pQCD result when $p_T \sim M$. The situation in Figure 4 can be understood by noting that shadowing in the resummed transverse momentum distributions is sensitive to the scale used to describe the nuclear effects on the parton distribution function and that the shadowing effect is re-distributed by resummation.

In summary, the shadowing effects in the p_T distribution of gauge bosons at RHIC and LHC are sensitive to the scale of the nuclear parton distribution. Therefore, the transverse momentum distribution of gauge bosons at LHC in $Pb + Pb$ collisions can provide a further test of our understanding of the nuclear parton distributions.

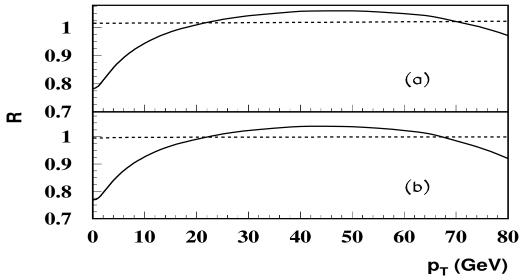

Fig. 4. (a) The isospin ratio, R_{iso} defined in Eq. (10) (dashed line) and the shadowing ratio, R_{sh}, defined in Eq. (11) (solid line) for Z^0 in $Pb + Pb$ collisions at $\sqrt{s} = 5.5$ TeV; (b) same as (a) for $W^{\pm}$ production.

5. Enhanced power corrections in nuclear collisions

We have seen that the effect of power corrections on the resummed cross section is very weak in pp collisions at both RHIC and LHC. In pA and AB collisions, power corrections will be enhanced due to rescattering in the nucleus. In this Section we discuss the enhancement of power corrections in nuclear collisions.

As $\bar{g}_2$ represents the effect of the partons' non-vanishing intrinsic transverse momentum, it should not have a strong nuclear dependence. On the other hand, g_2 arises as a result of dynamical power corrections, and should be enhanced by the nuclear size, i.e. proportional to $A^{1/3}$. Considering the enhancement, we get $G_2 \sim 0.8$ GeV^2 for $p + Au$ and $G_2 \sim 1.5$ GeV^2 for $Pb + Pb$ reactions.

In order to study the effects of power corrections, we now define $R^{sh}_{G_2}$ in nuclear collision as follows:

$$R^{sh}_{G_2}(p_T) \equiv \frac{d\sigma^{(G_2,sh)}(p_T, Z_A/A, Z_B/B)}{dp_T} \Big/ \frac{d\sigma^{(sh)}(p_T, Z_A/A, Z_B/B)}{dp_T} \ , \qquad (12)$$

where the numerator represents the result of the full calculation, with isospin effects, shadowing, and power corrections taken into account, and the denominator was introduced in connection with Eq. (11) and contains no power corrections ($G_2 = 0$).

Our calculations show that the effects of power corrections are enhanced about three times in $p + Au$ collision relative to pp collisions. However, even for $p_T \sim 0$, the effect of power corrections is only about 10%, and for $p_T > 2$ GeV, the effect remains under 5%. Thus the effect of power corrections is weak in $p + Au$ collisions at RHIC. As for the situation at LHC in $Pb + Pb$ collisions, displayed in Figure 11, the effects of power corrections appear to be enhanced by a similar factor (about three) from pp to $Pb+Pb$ collisions at LHC. The reason for the similar enhancement is the interplay of the higher energy and the larger value of G_2 mentioned above. In any case, the enhanced power corrections remain under 3% in the [0,80] GeV p_T interval for $Pb+Pb$ at LHC. The results for Z^0 production are similar to those for $W^{\pm}$ production.

6. Discussion and conclusion

We have demonstrated that the predictive power of a resummed pQCD calculation for gauge boson production is very good at RHIC and excellent at LHC, because the dependence of the cross sections on the non-perturbative input is weak. This makes $W^{\pm}$ and Z^0 production reliably calculable at the energies considered. On the experimental side, $W^{\pm}$ and Z^0 production should be an early observable at LHC (with sufficiently high production rates) in both pp and nuclear collisions. At RHIC, production rates may remain on the low side, in particular in pp collisions. In all cases, the cross sections peak at relatively low transverse momenta, and we calculate the peak position for all systems considered.

We have examined the effects of the isospin composition of nuclei and of shadowing in nuclear collisions. We find that isospin effects are modest in $W^{\pm}$ and Z^0 production at the energies considered, while shadowing is relatively unimportant at RHIC, but plays an important role at LHC in shaping the transverse momentum distributions. This comes about because of the sensitivity of shadowing effects to the scale of the parton distribution functions. We also studied the magnitude of power corrections in pp and nuclear collisions. Power corrections are small in pp collisions, and, even though part of these corrections is enhanced in nuclear collisions by a factor of $A^{1/3}$, they remain below 10% (even at very low transverse momenta) in AB reactions.

As indicated by the above observations, the resummed pQCD formalism yields accurate results for $W^{\pm}$ and Z^0 transverse momentum distributions at RHIC and LHC. The production of gauge bosons can therefore serve as a further test of the nuclear parton distributions. In more general terms, $W^{\pm}$ and Z^0 production at RHIC and LHC provides a bench mark test of resummed pQCD for pp and nuclear collisions at these energies. We hope that our predictions will soon be compared to data.

Acknowledgments

We thank T. Hallman, D. Keane, and R. Vogt for stimulating discussions and J.W. Qiu for a careful reading of the manuscript. This work was supported in part by the U.S. Department of Energy under Grant No. DE-FG02-86ER-40251 and by the NSF under Grant INT-0000211.

References

1. T. Affolder *et al.*, CDF Collaboration, Phys. Rev. Lett. **84**, 845 (2000).
2. B. Abbott *et al.*, D0 Collaboration, hep-ex/0010026.
3. J.C. Collins and D.E. Soper, Nucl. Phys. B **193**, 381 (1981); Erratum **213**, 545 (1983); **197**, 446 (1982).
4. J.C. Collins, D.E. Soper and G. Sterman, Nucl. Phys. B **250**, 199 (1985).
5. J. Qiu and X. Zhang, Phys. Rev. Lett. **86**, 2724 (2001); Phys. Rev. D **63**, 114011 (2001).
6. J. Qiu and G. Sterman,hep-ph/0111002, to appear in the Proceedings of the Hard Probe Collaboration.
7. J. Qiu and X. Zhang, hep-ph/0109210, to be appear in Phys. Lett. **B**.
8. R. Vogt, Phys. Rev. **C64** 044901(2001).
9. R.K. Ellis, D.A. Ross and S. Veseli, Nucl. Phys. **B503** 309 (1997).
10. R.K. Ellis and S. Veseli, Nucl. Phys. **B511** 649 (1998).
11. D. Appell, G. Sterman, and P. Mackenzie, Nucl.Phys. **B309**, 259 (1988).
12. G. Parisi and R. Petronzio, Nucl. Phys. **B154**, 427 (1979).
13. X. Zhang and G. Fai, in preparation.
14. R. K. Ellis, W. J. Stirling, and B. R. Webber, *QCD and Collider Physics*, Cambridge, England, 1996.
15. H. L. Lai et al., Eur. Phys. J. C **12**, 375(2000).
16. X.N. Wang and M. Gyulassy, Phys. Rev. D **44**, 3501 (1991).
17. S. Li and X.N. Wang, nucl-th/0110075.
18. K.J. Eskola, V.J. Kolhinen, and C.A. Salgado, Eur. Phys. J. C **9**, 61 (1999).
19. M. Hirai, S. Kumano, and M. Miyama, Phys. Rev. D **64**, 034003 (2001).
20. K.J. Eskola, H. Honkanen, V.J. Kolhinen, and C.A. Salgado, hep-ph/0201256 (2002).
21. C.T. Davies, B.R. Webber and W.J. Stirling, Nucl. Phys. **B256**, 413 (1985).